Journal of Petroleum
Science and Technology

DIAGENESIS AND RESERVOIR QUALITY EVOLUTION OF SHELF-MARGIN SANDSTONES IN PEARL RIVER MOUTH BASIN, SOUTH CHINA SEA

Lyu Chengfu[1], Chen Guojun[1]*, Du Guichao[1,2], Zhang Gongcheng[3], Zheng Sheng[1,2], and Li Chao[1,2]

[1] Key Laboratory of Petroleum Resources Research, Institute of Geology and Geophysics, Chinese Academy of Sciences, Lanzhou 730000, China
[2] University of Chinese Academy of Sciences, Beijing 100049, China
[3] Research Institute of China National Offshore Oil Corporation, Beijing 100027, China

ABSTRACT

A study of the diagenetic evolution of sandstones from Panyu low-uplift in the Pearl River Mouth Basin was carried out to unravel the controls on shelf margin sandstone reservoir quality. The reservoir rocks, Oligocene volcanic clastic sandstones of the Zhuhai Formation, have a burial depth of 2765 to 3440 m. 70 samples were studied using the granulometric analyses, X-ray diffraction (XRD) analyses, porosity and permeability measurements, SEM observations, and mercury porosimetry measurements. The sandstones are fine- to medium-grained lithic sub-arkose, sub-litharenite, and sub-arkose with an average framework composition of $Q_{72}F_{13}L_{15}$. High content and strongly altered volcanic rock fragments are the most important detrital components. In this work, typical diagenetic processes such as compaction, VRF (volcanic rock fragments) and feldspar dissolution, carbonate cements, quartz overgrowth, and clay cements are observed. Cements in eodiagenesis stage mainly include clay coating, early calcite and siderite. The main mesogenetic cements include kaolinite, ankerite, and minor quartz. The dissolution of VRF, feldspar, and carbonate cements is the most distinguishing feature which had controlled porosity and permeability. Carbon and oxygen isotopes were measured to discuss the carbon sources for precipitation and diagenetic temperatures of carbonate cements extensively developed in sampled intervals. Pore types in the analyzed samples change from a mix of primary to secondary pores. Primary pores have been destroyed by mechanical compaction or occluded by quartz, clay, and carbonate cements. Secondary pores were generated by the dissolution of VRF and feldspars during burial history. Its volume varied from trace to 8% and greatly improved the porosity of sandstones with increasing burial depth. Porosity varies from 4% to 20% in this work and is the highest for the samples where carbonate cement contents are low and dissolution is well developed.

Keywords: Sandstone Diagenesis, Reservoir Quality, Carbonate Cement, Compaction, Panyu Low-uplift, Pear River Mouth Basin

***Corresponding author**
Chen Guojun
Email: gjchen@lzb.ac.cn
Tel: +86 931 496 0908
Fax: +86 931 496 0916

Article history
Received: January 02, 2013
Received in revised form: October 08, 2013
Accepted: November 18, 2013
Available online: March 10, 2014

Journal of Petroleum Science and Technology **2014**, 4(1), 01-19 http://jpst.ripi.ir

INTRODUCTION

The Panyu low-uplift is one of the most important oil production and petroliferous areas in Pear River Mouth Basin. It lies on the shelf of South China Sea with a water depth of less than 300m. Several gas fields were discovered in this area since 2001 [1], indicating that the Panyu low-uplift has great hydrocarbon potential [2]. Although big progress was made in oil-gas explorations, limited drillings were carried out in the studied area and knowledge of diagenesis, petrophysical properties, porosity evolution, and controls of diagenesis on reservoir quality is still limited. So, the study of reservoir characterization in reservoir sandstones in Panyu low-uplift is necessary.

Reservoir quality assessment is one of the key elements on target sandstone reservoir prospectivety during hydrocarbon explorations [3-7]. Detailed understanding of reservoir quality and factors that control reservoir quality is important and essential to assist with the reservoir quality prediction and petroleum explorations [8-11]. In this study, a suite of deltaic sandstones from four wells of Panyu low-uplift in the Pearl River Mouth Basin was investigated with aiming to examine the diagenetic features during burial, describing reservoir quality characteristics, analyzing porosity evolution, and determining factors that control shelf-margin sandstones reservoir quality. We hope that the better understanding of the reservoir quality in the shallow water area of the Panyu low-uplift could help further exploration in this area and give an insight into the adjacent deep water prospects of the adjacent Baiyun Sag in Zhu II depression.

EXPERIMENTAL

Geological Setting

The Pearl River Mouth Basin (PRMB) is a passive continental margin basin and is composed of three sub-basins [12-14], including the Zhu I depression, the Zhu II depression, and the Zhu III depression. It is located in the northern continental shelf of the South China Sea, covering about 17.5×10^4 km^2. The geological evolution of the basin can be divided into three main tectonic stages, namely (1) rifting stage in the late Cretaceous period-the early Oligocene Epoch, (2) depression stage during the late Oligocene-the early Miocene, and (3) block faulting stage from the late Miocene to the present [12].

The study area, Panyu low-uplift, is situated in the middle of PRMB [15,16]. It lies in the middle part of CUB and is bounded by Baiyun Sag in Zhu II depression to the south and Zhu I depression to the north (Figure 1). Average water depth is 200 m. Eight formations from the bottom to the top have been recognized (Figure 2). The burial and thermal histories of the sandstones from Panyu low-uplift is shown in Figure 3. Gas reservoirs are developed mainly in Zhujiang, Hanjiang, and Yuehai formation [17]. Thick and extensively distributed lacustrine mudstone in the Eocene-Oligocene has been identified as the main source rock in the adjacent Baiyun sag [16,18,19]. There are four important Cenozoic tectonic events in the development and evolution of Panyu low-uplift:

1) Early Eocene-middle Eocene. Affected by the first episode of Zhuqiong movement, the south of PRMB experienced strong rifting and a series of separate deep sub-basins were formed. In this stage, Wencang formation in the Panyu low-uplift was deposited and mainly characterized by the deposits of alluvial fan-fluvial-lake facies.

2) Middle Eocene-early Oligocene. Affected by the second episode of Zhuqiong movement, the PRMB was uplift and further extensionally faulted. The area of lacustrine basin expanded in this period and Enping formation was deposited; the sedimentary environments are stream plain-

delta-lake facies in Panyu low-uplift. The strata of Enping formation are also important source rocks in PRMB.

3) Late Oligocene-middle Miocene, Nanhai movement, the strongest tectonic movement that PRMB experienced, caused regional up-lifting and erosion, resulting in regional unconformity in PRMB. In this stage, water level became shallower and Zhuhai formation was deposited; the sedimentary environments are delta, littoral facies. The sea floor of South China Sea spread in about 30 Million years and was also affected by the global increase of sea level. PRMB entered an entire subsidence stage and deposited thick strata of Zhujiang formation; the sedimentary environments are mainly delta, shallow marine facies. Reefs, shoal, and carbon-ate rocks were developed on the margin of uplifts or platforms.

4) Middle Miocene-late Miocene. Affected by Dongsha movement, the area was completely covered at this stage. Deposits of Hanjiang-Yuehai formation in the north depression zone of PRMB are mainly delta-neritic facies, while continental shelf-upper to continental slope deposits are present in the south depression zone.

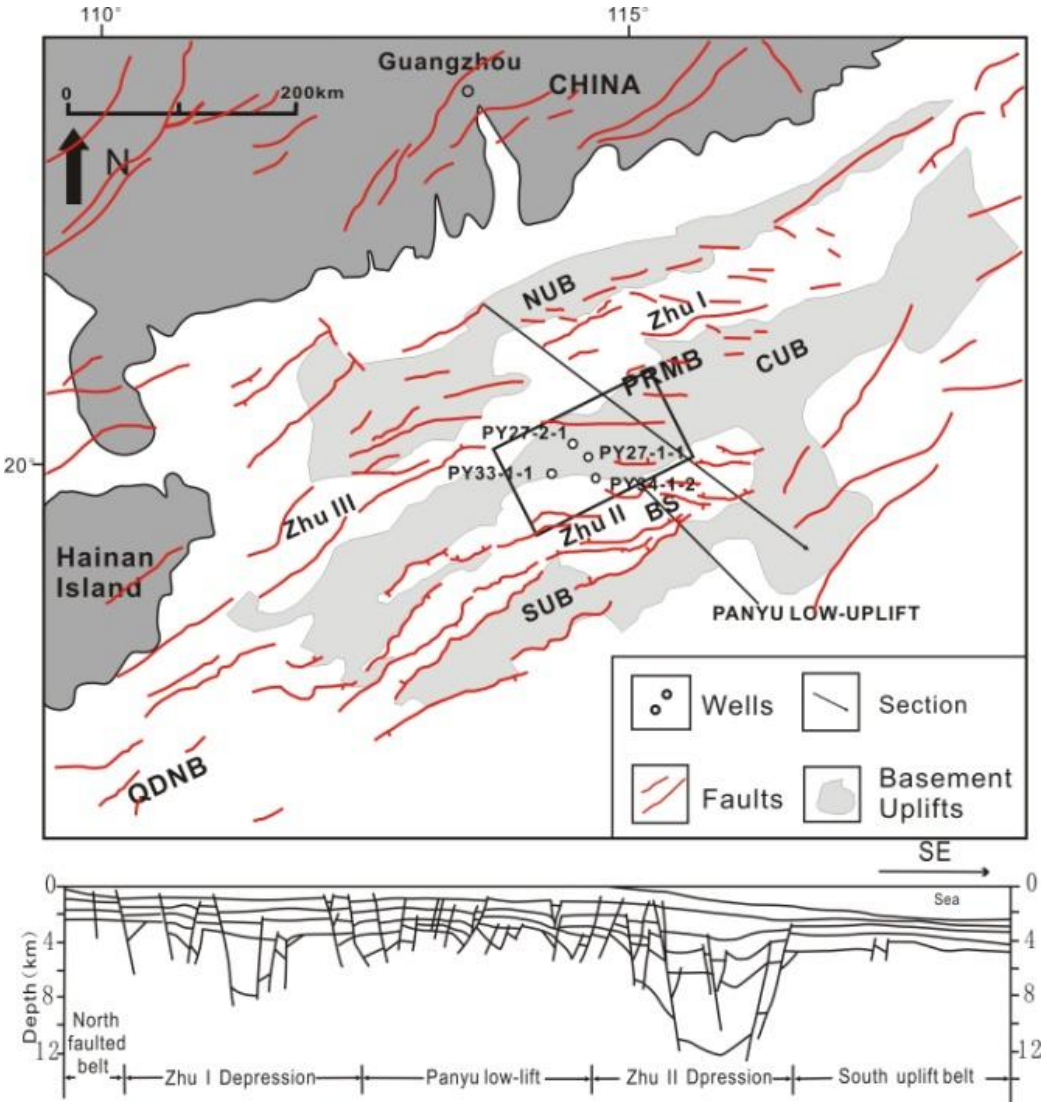

Figure 1: Location map of the Pear River Mouth Basin and the wells included in this study. PRMB: Pearl River Mouth Basin; QDNB: Qiongdongnan Basin; Zhu I: Zhu I Depression; Zhu II: Zhu II Depression; Zhu III: Zhu III Depression; NUB: Northern Uplift Belt; CUB: Central Uplift Belt; SUB: Southern Uplift Belt; BS: Baiyun Sag [15].

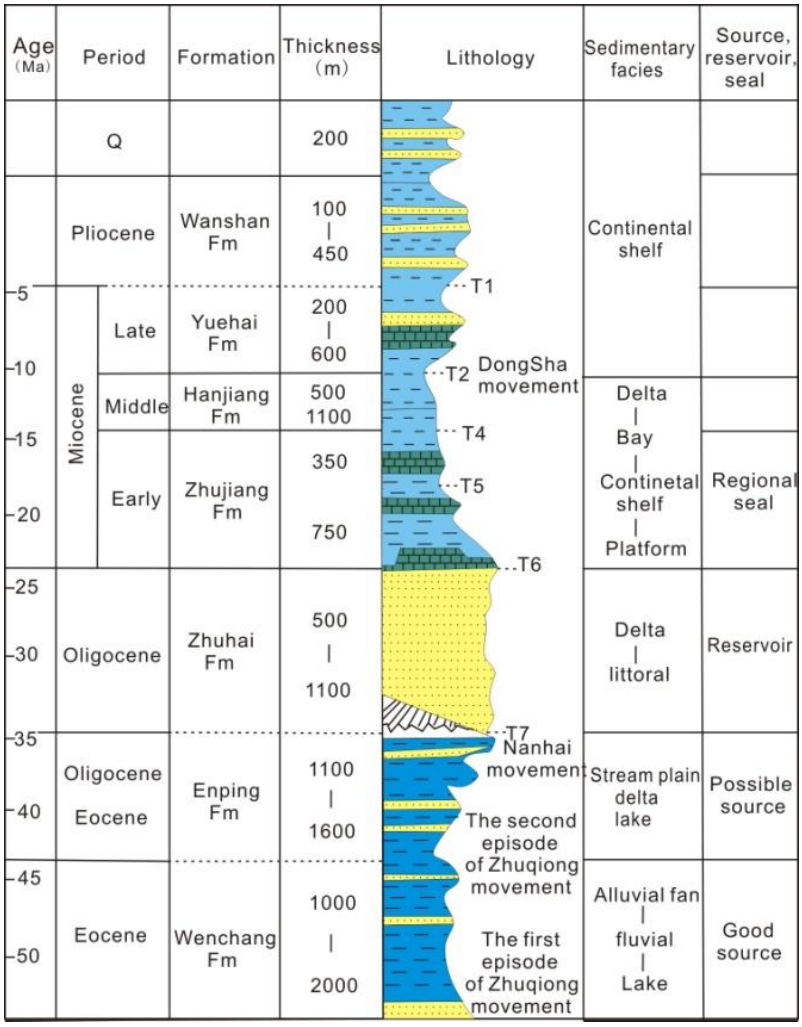

Figure 2: Generalized stratigraphic column of the Pearl River Mouth Basin modified from Zhang et al. [1]

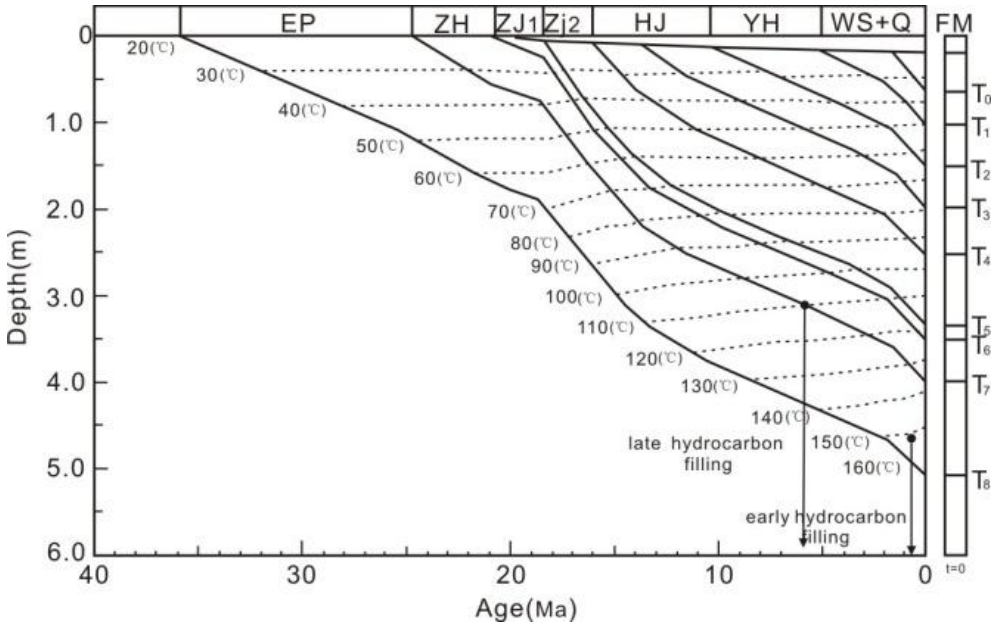

Figure 3: Diagram of burial-thermal history and time of hydrocarbon fillings for Panyu low-uplift (modified after Pang et al.). EP: Enping; ZH: Zhuhai; ZJ: Zhujiang; HJ: Hanjiang; YH: Yuehai; WS: Wanshan [8].

Samples and Methodology

A total of 70 core samples from Zhuhai formation in four wells in the studied area including 15 samples from well PY34-1-2 (3348.63-3386 m), 5 samples from well PY27-2-1 (3028.5-3034.6 m), 25 samples from well PY27-1-1 (2765.5-2783.06 m and 3221.7-3244.78 m), and 19 samples from well PY33-1-1 (3401.54-3438.2m) were taken from the main reservoir intervals. Before sampling, the detailed observation and description of cores were carried out.

The samples were impregnated with blue dye resin before thin section preparation to highlight porosity and assist the observation of pore types, features, distribution, and relationship with framework grains. Thin sections were stained with the mixed solution of alizarin red and potassium ferricyanide to distinguish carbonate minerals. Carbonate and clay minerals of 42 samples were analyzed by X-ray diffraction using a Philips PW3710 X-ray Powder Diffractometer and supported by scanning electron microscope (SEM) observation, aiming to characterize cement morphology, pore geometry, and diagenetic relationships. The grain size and rock compositions (detrital and authigenic components) of 22 representative samples were performed by counting 500 points per thin section. Petrophysical properties were determined from 35 samples using conventional helium porosimetry and klinkenberg-corrected gas permeametry by Research Institute of Qinghai Oilfield, CNPC.

The stable carbon and oxygen isotopes of carbonate cements of 18 samples were analyzed. The analysis was performed on calcite, dolomite, ferro-dolomite, and siderite-cemented sandstone samples. The samples were crushed and ground as fine as powder (<100 mesh) prior to analysis. Then, 100% phosphoric acid was dropped into sample powder at 25 °C for 36 hours to let pure calcite samples extract CO_2 from the calcite fraction, then at 50 °C to obtain CO_2 from ferriferous calcite, and at 100 °C to obtain CO_2 from ankerite. Isotopic composition was analyzed on a Finnigan MAT252 stable -isotope ratio mass spectrometer in the Geochemistry Department, the Test Center of Lanzhou Branch, Chinese Academy of Sciences. Isotope values were reported in standard delta notation as per mil (‰) difference from the PDB standard. Replicate measurements of the internal laboratory standard gave a total analytical precision of ±0.02‰ for both carbon and oxygen measurements [10,20]. The equations of Craig were used to calculate the precipitation temperature of siderite, calcite, and ankerite [21].

RESULTS AND DISCUSSION

Petrographic Features and Mineralogical Compositions

Reservoir sandstones in well PY34-1-2 and well PY27-2-1 are mostly classified as fine- to medium-grained lithic sub-arkose, and a few as sublitharenite. The average framework composition of the sandstones is $Q_{69}F_{13}L_{18}$ (Figure 4). Content of detrital quartz grains is higher than 60%, lithic grains are less than 20%, and feldspar grains are less than17% (Table 1). Lithic grains are dominated by volcanic (5-19%), minor chert, quartz schist, and phyllite (5%). Volcanic lithics are slightly sericitizated. Diagenetic components are characterized by minor quartz overgrowth (0.5-1.1%) and carbonate cement (average 5%). The delta front sandstones are fine- to medium-grained and moderately sorted [18].

Sandstones taken from well PY27-1-1 are lithic sub-arkose, with a few as sub-arkose. They are fine- to medium-grained and poorly to moderately sorted.

Table 1: Average detrital composition and main diagenetic constituents in the deltaic front sandstones (%)

Detrital and Diagenetic Constituents	Well PY34-1-2	Well PY27-2-1	Well PY27-1-1/a	Well PY27-1-1/b	Well PY33-1-1
Sample	15	5	9	16	19
Quartz	65.9	71.7	76	71.8	76.5
K-feldspar	12.5	12.7	12.6	12.2	14.1
Plagioclase	1.1	1.4	1.4	2.7	1.1
Volcanic Rock Fragments	16	11	9.5	9.2	9.8
Metamorphic Rock Fragments	5.6	4.7	2.1	4.5	3.9
Chlorite	0	0	0.7	0.8	0
Kaolinite	2.1	1.2	0.9	0.65	1.8
Illite	1.3	2.6	0.85	0.56	1.9
Smectite	0	0	trace	0	0
Siderite	0	0.4	trace	0.2	0
Calcite	4.6	1.5	9.6	4.5	9.5
Dolom/Ankerite	1.4	1.2	1.3	0.4	1.5
Intergranular Siderite	0.2	0.4	0.2	0.2	0.3
Quartz Overgrowth	0.5	1.1	0.5	0.9	0.8
Pyrite	trace	0	trace	trace	0

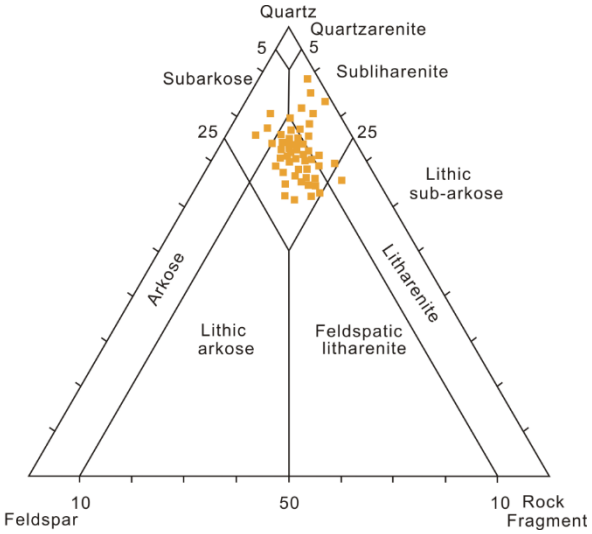

Figure 4: Quartz-feldspar-lithic grain ternary plot showing the composition of the detrital grains of the sandstones under McBride's 1963 classification scheme [22]

The average framework composition of the sandstones is $Q_{76}F_{13}L_{11}$ in the upper interval and $Q_{72}F_{12}L_{16}$ in the lower interval. Lithic grains are more abundant in the lower interval and are mainly volcanic lithics (5-15%) (Table 1). The samples of well PY27-1-1 are characterized by chlorite cements (0.7%), carbonate cements (2-15%), and quartz overgrowth (0.5-0.9%).

The samples of well PY33-1-1 are classified as lithic sub-arkose, with a few sub-arkose, having an average framework composition of $Q_{77}F_{14}L_{9}$. The sandstones are fine- to medium-grained and poorly to moderately sorted. Lithics are mainly volcanic (9.8%) and strongly sericitizated. Characterized diagenetic components are carbonate (5-15%) and quartz overgrowth (0.5-1%) (Table 1).

Diagenetic Processes

Compaction and Pressure Dissolution

These sandstones are moderately to strongly affected by compaction during burial. During compaction, mica plates were moderately to strongly deformed. The stronger compaction occurred in lower samples of well PY33-1-1. Volcanic rock fragments were strongly deformed and squeezed in intergranular pore spaces

between quartz grains (Figure 5a), as indicated by the samples from the depth lower than 3400m. Grain contacts are mainly line and concave-convex contacts. Minor rigid quartz grains were rearranged and occasionally fractured. Pressure dissolution particularly occurs both along intergranular contacts and stylolites between quartz grains. Pressure dissolution not only reduces primary porosity, but also provides the solute which will precipitate around the grains as secondary overgrowth and will destroy intergranular pores.

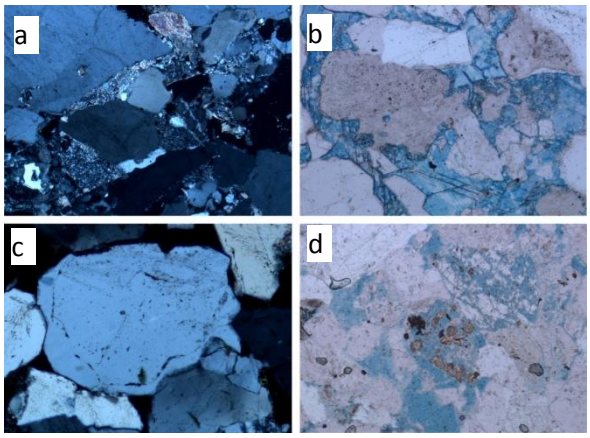

Figure 5: (a) Well PY34-1-2, (×50), 3349.86 m, E_3^2zh, strongly compacted sandstones. Ductile lithic grains were strongly deformed and squeezed into pore spaces; (b) Well PY34-1-2, (×100), 3381.91 m, E_3^2zh, ferro-dolomite fills intragranular pores and replaces quartz grains; (c) Well PY27-1-1, (×25), 3239.62 m, E_3^2zh, quartz overgrowth with dust lines between them; (d) Well PY27-2-1, (×50), 3143.75 m, E_3^2zh, dissolved pores generated by dissolution of volcanic debris.

Carbonate Cementation

Siderite

Siderite is typically less common in these sandstones, but it significantly shows diagenetic features. It occurs commonly as scattered crystals and concretions in fine- to coarse-grained sandstones (Figure 6b), which are poorly sorted and moderately compacted. Scattered crystals are developed as cements in filling intergranular pores and secondary pores formed by the dissolution of VRF and feldspars, generally indicating that siderite predates dissolutions. Also, siderite crystals are particularly embedded in ankerite concretions, showing that siderite precipitated before the development of ankerite. Siderite slightly replaces quartz grains in the sample taken from the depth of 3238.2 m in well PY27-1-1 and no quartz overgrowth can be seen around the quartz grains wrapped by siderite cements.

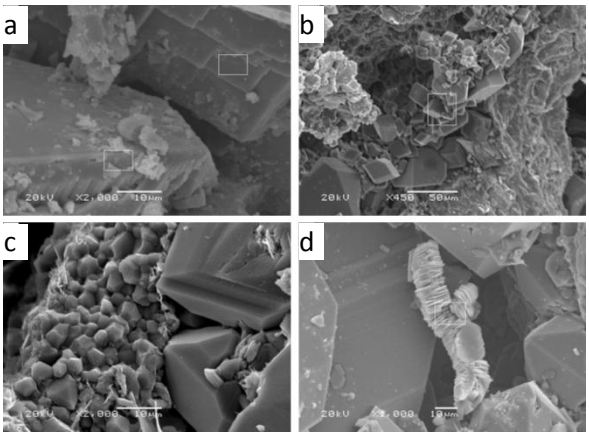

Figure 6: SEM images of sandstones;(a) Well PY34-1-2, 3348.63 m, E_3^2zh, well PY27-1-1, crystallized calcite cement; (b) Well PY27-1-1, 2781.12 m, E_3^2zh, siderite occurs as scattered crystals in intragranular pores; (c) Well PY34-1-2, 3368.32 m, E_3^2zh, authigenic quartz cements that fill intragranular space; (d) Well PY27-1-1, 3221.7 m, E_3^2zh, authigenic kaolinite and partly filling pores.

Siderite is created in minor amounts and is always embedded in ankerite concretions. The $\delta^{13}C$ value of siderite cement is -7.2‰ and the $\delta^{18}O$ value is -11.4‰ (Table 2). The relatively light value indicates that the source of siderite cement was precipitated from the addition of organic matter decarboxylation. It was precipitated relatively late in diagenetic history and predated dissolution and parts of ankerite. The precipitation of siderite was at a reservoir temperature of 80 °C.

Calcite

Calcite cements have a heterogeneously distribution and tend to have a two-stage development in this study.

Table 2: Isotopic ratios of representative carbonate cements and temperatures calculated by Craig [21]

Sample No.	Depth (m)	Cement type	$\delta^{13}C$ (PDB)	$\delta^{18}O$ (PDB)	Temperature (°C)
PY34-1-2-01C	3348.63	Calcite	-7.6	-12.2	86
PY34-1-2-02C	3349.4	Calcite	-6.5	-13.4	95
PY34-1-2-03C	3349.86	Calcite	-6.1	-12.1	85
PY34-1-2-04C	3354.02	Calcite	-6.2	-11.2	79
PY34-1-2-05C	3355.4	Calcite	-6.8	-12.1	85
PY34-1-2-06C	3355.98	Calcite	-6	-13	92
PY34-1-2-13C	3381	Calcite	-5.5	-14.9	106
PY27-2-1-02C	3028.8	Calcite	-6.3	-13.1	92
PY27-2-1-03C	3034.5	Siderite	-7.2	-11.4	80
PY27-1-1-08C	2781.12	Calcite	-5.4	-13.5	95
PY27-1-1-09C	2783.06	Calcite	-5.9	-12.2	86
PY27-1-1-10C	3221.7	Calcite	-4.8	-12.5	88
PY27-1-1-16C	3230.75	Ankerite	-10.4	-12.3	86
PY27-1-1-23C	3241.32	Calcite	-8.9	-13.7	97
PY33-1-1-08C	3433.3	Calcite	-4.5	-9.1	64
PY33-1-1-10C	3434.1	Calcite	-5.4	-11.9	84
PY33-1-1-11C	3435.5	Ankerite	-6.2	-8.9	63
PY33-1-1-13C	3437.91	Ankerite	-7.4	-6.8	50

Early cementations are represented by cements in samples at the depth of 2771.68 m in well PY27-1-1 and at the depth of 3433.3 m in well PY33-1-1. The sandstones are fine- to medium-grained and poorly sorted with a pre-calcite basal cemented, which shows a pre-compactional cementation. Calcite occurs as basal cements with a high content of 25-30% by point-counting data in thin sections. The formation time of this calcite is earlier than the other diagenetic alterations. Framework grains were wrapped in calcite concretions and no quartz overgrowth, dissolution of VRF and feldspar, and chlorites were present.

Late calcite cementations are characterized as pore-fillings and concretions in poorly sorted, fine sandstones (Figure 6a). It significantly shows variation in distribution from sample to sample and has a content which ranges from 2% to 14% (average 5-6%). Calcite cements occurs in replacing quartz grains and quartz overgrowth are present, showing that they precipitated after the development of quartz overgrowths.

The $\delta^{13}C$ values of calcite cements ranges from -4.5 to -8.9‰ and $\delta^{18}O$ from -9.1to 14.9‰ (Table 2). Early calcite cements precipitated earlier tend to have heavier $\delta^{13}C$ values. The C and O isotopic value indicates that the source is mostly related to the oxidation or decarboxylation of organic matter and has a negative relationship with inorganic sources, because various studies have reported that the $\delta^{13}C$ values of the normal marine carbonate rocks and cements vary between -4‰ and +4‰ (PDB) [20,22]. No dissolution of carbonate fragments as internal source of calcium and CO_2 was observed in this study [23]. Former studies show that with increasing burial depth, pressure and temperature increased to promote the evolution of organic matter in source rocks which will release part of carbon dioxide gases with lighter carbon isotope [20,24,25]. The lighter $\delta^{13}C$ composition was released, then dissolved into fluid and contributed to the formation of carbonate

cements. Also, having carbon dioxide gas been input into fluid, the environment was transformed into an acidic environment. When the acid entered the reservoir sandstones, it will dissolve the feldspar, lithic grains, and early carbonate cements to generate secondary pores (see Figure 5d) [20]. Calcite cement was precipitated at temperatures ranging from 64 °C to 106 °C calculated by the formula listed by Zhang [6], showing both early and late precipitations in diagenetic history [26]. In deep buried, source rocks reached a high maturity stage with high temperature and pressure. Therefore, hydrocarbon generation from source rocks reached its peak volume. Large volume of hydrocarbon infilling the sandstone reservoir caused the former acidic environment transformed into an alkaline environment and lighter ^{13}C-depleted materials were added for calcite precipitation.

Ankerite

Ankerite cement is extensively developed in the sandstones with its content less than calcite. It commonly occurs as pore-fillings and cements replacing framework grains. Pore-filling cements typically occur after effective compaction. Quartz grains, quartz overgrowth, and lithic grains are replaced by ankerite crystals in the sandstones (Figure 5b), indicating that this ankerite shows a characteristic of later development than quartz overgrowths. Small ankerite crystals also occur as cements filling in secondary pores formed by the dissolution of VRF and feldspars, characterizing that it precipitated later than the dissolution of VRF and feldspars in this study.

Three ankerite-cemented samples were picked to analyze carbon and oxygen isotope compositions. The $\delta^{13}C$ values of calcite cements ranges from -6.2 to -10.4‰ and $\delta^{18}O$ varies from -6.8 to -12.3‰ (Table 2). Ankerite was formed at reservoir temperatures ranging from 50 °C to 86 °C calculated by the formula listed by Zhang [6], indicating both early and late precipitations [26].

Quartz cements

The precipitation of quartz overgrowths occurs after effective burial and compaction. Quartz cements in the sandstones occur mainly as quartz overgrowths around quartz grains and isolated patches and are composed of small crystals and trace amounts of isolated quartz crystals which fill intergranular pore spaces (Figure 6c) or secondary dissolved pores. Discontinuous overgrowth is common. It occurs on quartz surface with a poorly defined boundary. Quartz overgrowths tend to be much more abundant in the deeper buried sandstones at the depth of lower than 3200 m. Particularly, the amount of quartz cement is greatly limited in samples that have a high content of ductile lithic grains. Ductile-lithic contents in well PY34-1-2 and the lower sampled interval of well PY27-1-1 are 6-13.5 vol.% and 5-17 vol.% respectively, with quartz overgrowth of trace to 1.4 vol.% and 1.5 vol.% respectively. Ductile-lithic grains are 3-5 vol.% and much lower in the samples of well PY33-1-1, but they tend to have much higher quartz overgrowth of 2.3 to 5 vol.% . Ductile contents appear to control the amount of quartz cement because ductile lithic grains are deformed and become closely contacted with the surface of rigid grains as compaction increases. In some cases, ductile grains are squeezed into intergranular pore spaces.

Generally, quartz overgrowth on detrital quartz grains is inhibited by well developed chlorite cements (Figure 7a). Quartz overgrowths are present when quartz grains are not coated by chlorite rim or chlorite rim is thin or discontinuous. Well developed chlorite rims play the role of effective barriers to inhibit quartz overgrowth [27].

The sources of silica may have been from three sources, including (1) the pressure dissolution of detrital quartz along intergranular contacts and discrete stylolites (Figure 5a), (2) the dissolution

or alteration of detrital silicates, mainly volcanic rock fragments (Figure 5d), and (3) the illitization of detrital and authigenic kaolinite (Figure 8a).

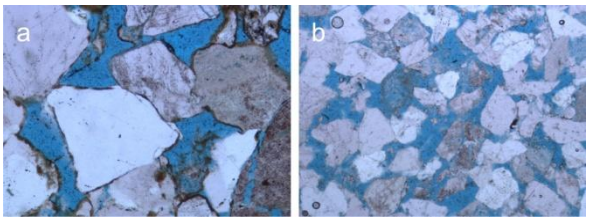

Figure 7: (a) Well PY27-1-1, (×50), 3432.14 m, E_3^2zh, chlorite rims and intergranular pores, grain contact and point-line contact; (b) Well PY27-2-1, (×25), 3028.80 m, E_3^2zh, intergranular and intragranular pores, rather open pore-structures for sandstones of delta facies.

In common, the intergrowth of quartz is occurred by fibrous illite, kaolinite, and chlorite (Figure 8c). Moreover, siliceous cements sourced from the dissolution of feldspar are indicated by the common occurrence of inter-growth of quartz with fibrous illite, kaolinite, and chlorite (Figure 8c).

Clay Minerals

Clay minerals identified in the sandstones of the studied area include illite, kaolinite, chlorite, and smectite. As determined by thin section observations, SEM and XRD analysis, Illite and kaolinite are the most common clay minerals and they are present in almost all the analyzed samples. The presence of chlorite and smectite is limited.

Kaolinite occurs as aggregates stacked by pseudo-hexagonal crystals replacing feldspar grains. It fills the dissolved pores and occurs adjacent to quartz overgrowth. Kaolinite also occurs as booklets (15 µm across) in filling intergranular pore spaces and associates with quartz overgrowth (Figure 6d). Although there is no clear evidence on the material source for its precipitation, it preferentially occurs associated with quartz overgrowth. In some cases, kaolinite occurs as isolated and disordered crystals (5 µm) engulfed by illite crystals. Kaolinite has a highly irregular distribution and its amount varies from sample to sample. It composes up to about 4% of the rocks and occupies up to about 45% of the clay minerals.

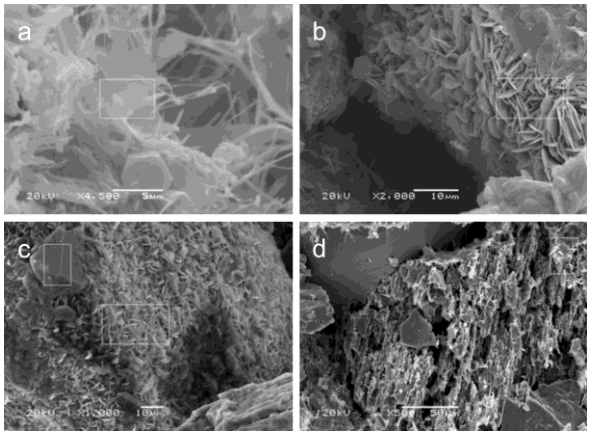

Figure 8: SEM images of sandstones;(a) Well PY27-2-1, 3630.25 m, E_3^2zh, fibrous illite crystals in deep buried sandstones; (b) Well PY27-1-1, 3244.78 m, E_3^2zh, fine-crystalline chlorite rims covering detrital quartz grains; (c) Well PY27-1-1, 3239.62 m, E_3^2zh, quartz overgrowth and chlorite coat covering quartz grains; (d) Well PY33-1-1, 3299.85 m, E_3^2zh, dissolution of feldspar generates abundant secondary pores.

Illite is found mostly in pore spaces and partly within the matrix. It is represented by three different texture types, namely (1) hair-like, radically disposed crystals (Figure 8a) which occur as pore-filling and pore-lining cement; (2) fibrous crystals; and (3) membranous structures, which occur as pore-filling and pore-lining cements. Illite forms up to about 5% of the rocks and forms up to 50% of the clay minerals. Sources of illite cement are mostly from the alteration of feldspar and VRF and smectites.

Chlorite cement is only found in the samples of well PY27-1-1 and the amount varies form 0.5-2%. A relationship between chlorite cement and higher porosity in the samples is observed in this study. Chlorite is present in three forms, namely pore-filling and pore-lining cements (<5 µm),

crystal aggregates filling within the pores and growing on the surface of detrital grains (Figure 8b and 8c, Figure 7a), and chlorite coatings which indicate a pre-compactional precipitation and are deformed between adjacent rigid grains as compaction increases. It is the most important type of clay minerals. Since other cements are inhibited by chlorite cements, detrital grains coated by chlorite are clean. Little or no quartz overgrowths are developed in samples when detrital grains are coated; it is only developed in spaces where chlorite rims are thin or discontinuous as shown in SEM images. VRF and feldspar grains are partially to completely dissolved in the samples without chlorite coatings. Hence the development of chlorite rims around detrital grains appears to have helped the prevention of the dissolution of VRF and feldspar grains by pore water. The development of chlorite rims has also helped the preservation of porosity by enhancing the mechanical strength of the detrital grains against mechanical compaction and pressure dissolution. Although no direct evidence for confirming the source of chlorite cement is shown, the dissolution of VRF must provide abundant Fe^{2+} and Mg^{2+} into pore waters to help the transformation of chlorite cements.

Smectite cements are minor in the studied sandstones according to the SEM evidence and XRD data and are mostly developed at the depths lower than 3000 m. Its content is in the order of traces in the most tested samples and is lower than 1% in the samples taken from the depths of 2765 m and 2768 m. The current work shows that smectite forms early in eodiagenesis and experiences illitization or dissolution. The illitization of smectite cements occurs when Al^{3+} and K^{+} are added into pore fluids. This reaction also releases abundant Si^{4+} as one possible source of quartz cement.

Diagenetic Sequence

Diagenetic process is closely related to porosity evolution, but the timing of different processes and their effects on porosity vary greatly during the burial history of reservoir sandstones. Therefore, detailed understanding of diagenetic sequence is helpful for finding the major controlling factors of reservoir quality and predicting reservoir qualities. Based on the above observations of diagenetic characteristics, the sequence of authigenic minerals, fabric features (contact of detrital grains and pore types, etc), evolution, coexisting relationship of authigenic minerals, hydrocarbon migration and emplacement, typomorphic minerals precipitated in acid and alkaline environment, the diagenetic environment, diagenetic phases, and diagenetic sequence of the reservoir sandstones have been constructed.

Sandstones buried at the depth of less than 3000 m in the Zhuhai formation are mainly in the A_1 stage of meso-diagenesis, while those buried at the depth of greater than 3000 m are in the A_2 stage of meso-diagenesis. Diagenetic environment in the first stage is strongly acidic and gradually switched to weakly acidic and finally weakly alkaline in the late stage. Diagenetic sequence in the reservoir sandstones is schematically illustrated in Figure 9. In summary, the diagenetic gradation of deltaic sandstones can generally be arranged as:

Compaction→ early clay coatings → early carbonate cements → organic acids invading → the dissolution of volcanic rock fragments and feldspars → kaolinite and quartz overgrowth → metaphase carbonate cements → hydrocarbonate emplacement → the displacement of quartz grains by late carbonate cements.

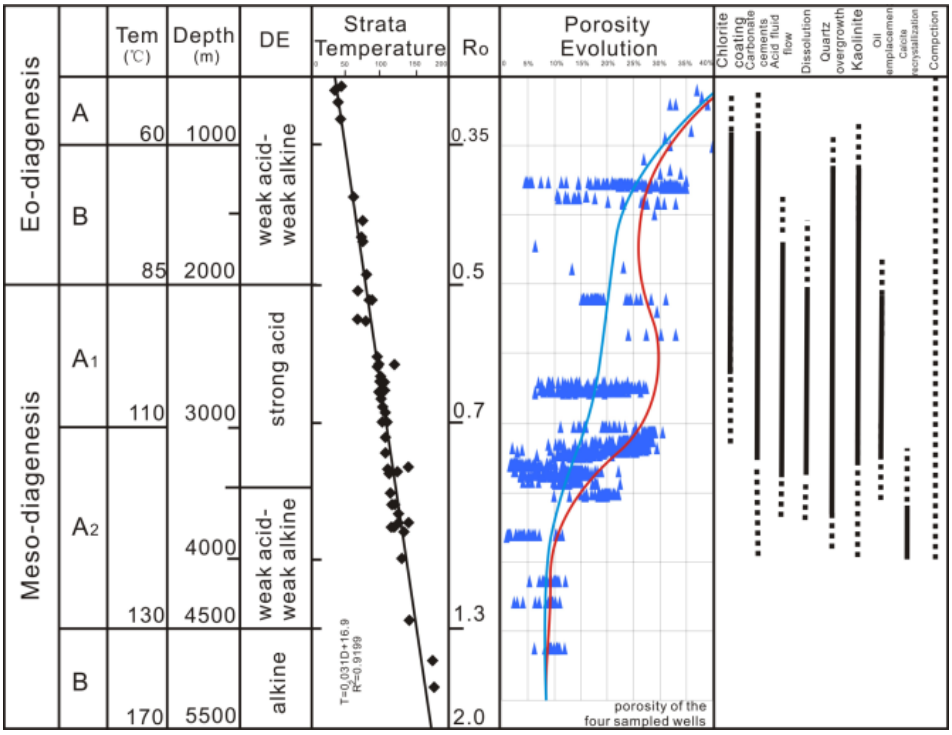

Figure 9: Paragenetic sequence for the main diagenetic processes occurring in the sandstones, as interpreted from petrographic relationships; DE: Diagenetic temperature; Tem: Temperature; Strata temperature was modified after Pang et al. [8].

Mechanical compaction and dissolution are the most important diagenetic features in the deltaic sandstones of Zhuhai formation. The sandstones experience typically medium mechanical compaction through burial history and multi-phase dissolution by acid fluid discharged by multiple set of source rocks. The A_1 stage of meso-diagenesis specifically has a strong acid environment with abundant organic acid in pore waters. Generally, in this stage, the complicated fluid-rock interaction is widely developed. Abundant secondary pores are generated by the strong dissolution of VRF and feldspars, and the formed secondary pore zone improves the connectivity of pores in this stage.

Petrophysical Properties

Pore Types

Pore types in the sandstones of Zhuhai formation include residual intergranular pore, intergranular dissolution pore, intragranular dissolved pore, intercrystalline pore fracture, and minor micropores in interstitial materials (Table 3). The most significant pore types are intergranular pore, intergranular dissolution pore, and intragranular dissolution pore. The average volume of intergranular pore varies from 14 vol.% to 42 vol.% (average 23 vol.%) of the total porosity. The secondary pores (including intergranular dissolution pore and intragranular pore) ranges from 55 vol.% to 84 vol.% (average 75 vol.%) of the total porosity. Micropore, intercrystalline pore, and fracture pore are volumetrically limited to a volume of 1-3% of the total porosity.

Porosity and Permeability

The reservoir quality analysis of sandstones obtained from the four wells shows that porosity ranges from 2.3%-25.4% (average 13.9%) and permeability varies from 0.07×10^{-3} md to 1310×10^{-3} md (average 133.9×10^{-3} md).

Table 3: Average values of sandstone pore types; Pore data are from thin-section database.

Pore types \ Well	PY34-1-2	PY27-2-1	PY33-1-1	PY27-1-1/a	PY27-1-1/b
Intergranular pore	14%	15%	25%	19%	42%
Intergranular Dissolution pore	73%	46%	64%	34%	48%
Intragranular Pore	11%	37%	9%	45%	9%
Intercrystalline \fracture\micropore	2%	3%	2%	2%	1%

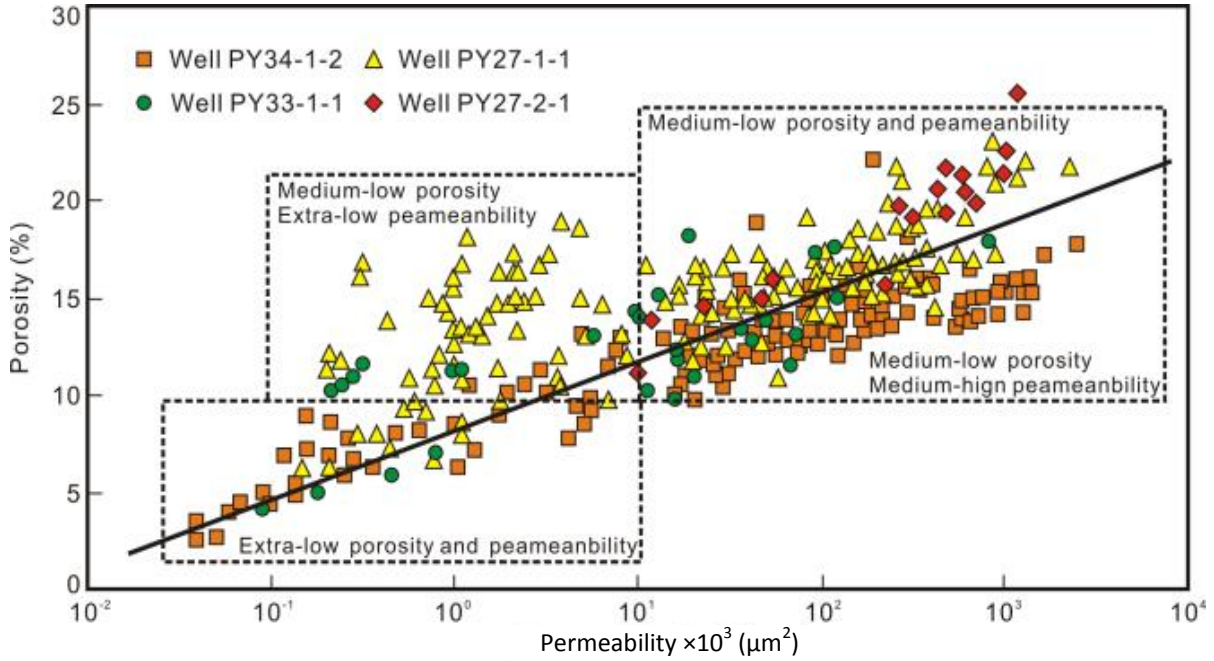

Figure 10: The relationship between measured porosity and permeability for the samples from Panyu low-uplift

From the total porosity and permeability data from Zhuhai formation, 16.5% of sandstones have a porosity smaller than 10%, 31.5% between 10% and 15%, 45.2% between 15% and 20%, and 6.8% between 20% and 25%. The value of permeability lower than 10×10^{-3} μm^2 reaches 42.4%; 23.3% of permeability values lie between 10×10^{-3} μm^2 and 100×10^{-3} μm^2; 19.2% of the values are between 100×10^{-3} μm^2 and 300×10^{-3} μm^2 and 15.1% are greater than 300×10^{-3} μm^2 (Figure 10).

Porosity Evolution

Based on the petrographic observations, diagenesis specifically controls reservoir quality, including mechanical compaction, dissolution, cementation, authigenic mineral filling, etc. Generally, mechanical compaction occurs through the entire burial history of sandstones and plays a major role in porosity reduction. Dissolution creates secondary porosity and permeability. It greatly improves sandstone reservoir quality in the studied area. Additionally, cementation (carbonate and quartz) caused the progressive loss of porosity and permeability during burial. Considering the different effects of major diagenetic processes on reservoir quality, porosity evolution can be divided into three stages as follows (Figure 9):

1) A stage of eodiagenesis; the burial depth of sandstones is lower than 1500m and is mainly in a weak alkaline diagenetic environments. In this stage, affected by overlying static pressure, porosity is sharply reduced because of the

rearrangement of detrital grains and the discharge of pore waters. Detrital grains become point contact. Pore type is mainly primary pore. In weakly alkaline diagenetic environments, early calcite and ankerite begin to precipitate and fill intergranular pores. The representative sample is sample from the depth of 2771.68 m and 3433.3 m respectively from well PY27-1-1 and PY34-1-2. The contents of carbonate cements are 20-30 vol.% with a pre-cemented porosity of 40-45% under thin-section. Early chlorites begin to precipitate when diagenetic temperature is less than 50 °C and before effective compaction starts. Intergranular pores are effectively preserved in sandstones with well-developed chlorite coatings. Generally, early mechanical compaction reduces porosity by 5-10% and early carbonate cements decreases porosity by 5-10%.

2) B stage of eodiagenesis—an early A_1 stage of meso-diagenesis; the burial depth of sandstones ranges from 1500 to 2500 m. Detrital grains are mainly point and point-line contact. Pores at this stage are mainly primary pores. Dissolution pores begin to develop with diagenetic environment gradually changed from a weakly alkaline to a weakly acidic environment. Mechanical compaction is enhanced by overburden sediments and greatly reduces porosity through burial. Carbonate cements continue to precipitate and fill intergranular pores and effectively reduce intergranular porosity. At this stage, clay minerals and quartz overgrowth begin to precipitate and are widely developed in the studied area, but with a limited effect on porosity reduction. Weak dissolution typically begins to occur as acid fluid entered the pore waters. Generally, mechanical compaction reduces porosity by 5-15% and carbonate cements decreases porosity by 5-25%.

3) A_1 stage-A_2 stage of meso-diagenesis; the burial depth of sandstones ranges from 2500 to 3500 m. Detrital grains are point-line and line contact. Diagenetic environments have switched from weakly acidic to strongly acidic. At this stage, the most characterizing feature is that organic acid discharged from low mature to mature organic matter is added into pore waters. They strongly dissolve VRF, feldspar, and early carbonate cements. Generally, mechanical compaction reduces porosity by 5-15% and cementation by 2-10%. While, strong dissolution greatly improves and increases porosity by 5-12%. A secondary porosity zone is developed in the depths interval between 2750 and 3500 m. This is the reason why reservoir quality in sandstones of Zhuhai formation is greatly improved.

Major Factors Controlling Reservoir Quality

Compaction and Porosity

Mechanical compaction is simple but plays a major role in reducing porosity (Figure 11). Obvious evidence of mechanical compaction in reducing porosity is shown. Correspondingly, porosity is lost during the processes of intergranular rearrangement, deformation of ductile grains, etc. Thin section studies show that grain contact evolves from separation to point to point-line and to line contact because of strong compaction from shallow to deep burial. This characteristic also indicates the relationship of porosity with burial depth. Thus porosity reduced by compaction can be divided into two stages, namely eodiagenesis (<2000 m) and meso-diagenesis (2000-3500 m). Average primary porosity in deltaic sandstones was assumed to be 40% immediately after deposition [28]. It tended to decrease intensively with increasing the depth of burial and relatively decreased from 40% to less than 25% in eodiagenesis. The rate of reduction in porosity by compaction was slower in meso-diagenesis than in eodiagenesis and became less than 20%.

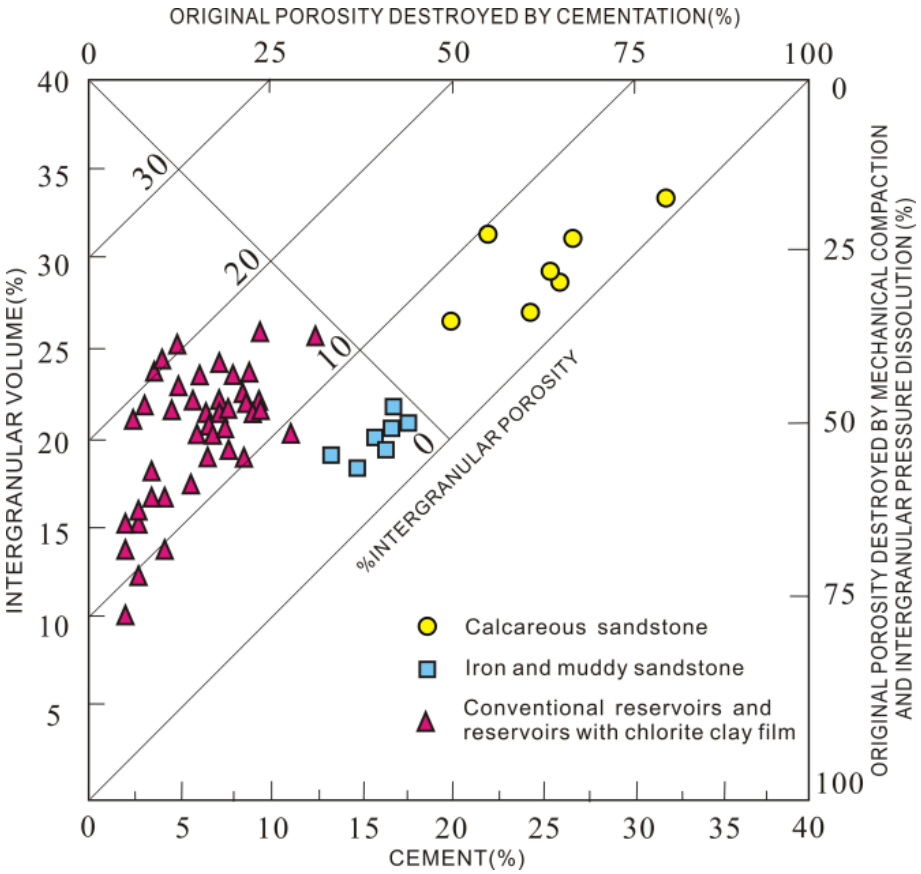

Figure 11: Plot of cement volume percent vs. intergranular volume percent of Panyu low-uplift sandstones (cf. Houseknecht [28]). Compaction and cementation had a similar importance in the destruction of porosity in the deltaic sandstones of Panyu low-uplift.

Dissolution and Porosity

Dissolution is the main factor generating secondary porosity, which plays a key role in porosity evolution. Thin section and SEM observations show that the content of unstable components is volumetrically high and can be classified into three categories including VRF (5-30%), feldspar (2-5%), and early carbonate cements (5-30%). In the studied area, dissolution begins in the B stage of eodiagenesis, and unstable constituents are dissolved when organic acid enters into pore water. In the A_1 stage of meso-diagenesis, abundant organic acid is discharged by the evolution of source rock and is added into pore waters. The unstable constituents are strongly dissolved in the acid environment. The relationship between porosity and depth shows that a secondary porosity zone is developed in the depth interval between 2750 and 3500 m. In this interval, intergranular dissolution pore and intragranular dissolution pore are abundantly generated. Secondary porosity generated by dissolution may reach 5-15% according to thin section database.

Carbonate Cementation and Porosity

Carbonate cement is a main factor in controlling sandstone reservoir properties (Figure 11) and may have a strong influence on fluid flow [22,29]. Carbonate cements are widely developed in sandstones from the four wells (Figure 12). The effects of carbonate cements on porosity are evidently observed by the relation between the amounts of the cement and the measured porosity and permeability (Figure 13). When the content of carbonate cement is higher than 15%, the porosity is normally lower than 10%.

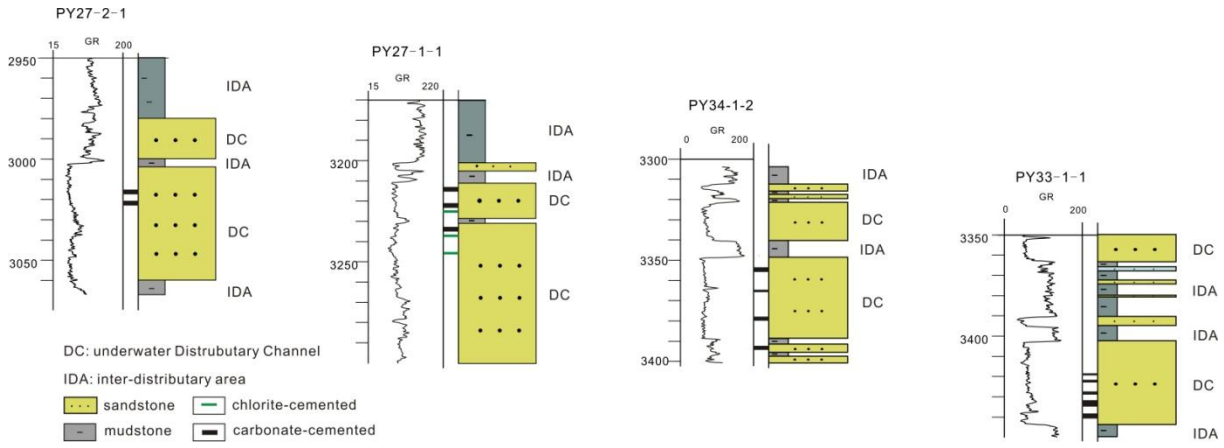

Figure 12: Sampled intervals from well PY27-2-1, PY27-1-1, PY34-1-2, and PY33-1-1; Lithology and macro-sedimentary facies are interpreted based on log response and core samples taken from the intervals.

On the other hand, when its content is less than 10%, the porosity may reach 25%. An inverse relationship is also seen between carbonate content and permeability (Figure 13b). Carbonate cements occur in the thickness range of 0.5 m to lower than 4 m and act as a main porosity reducing factor compared with the other cements (Figure 12). Fine-grained sandstones are generally more favorable for the development of carbonate cements than the coarse-grained sandstones. Thin sandstones have higher carbonate cements than thick sandstones. Further, thick sandstones tend to have carbonate cements in the upper and lower ranges of the intervals. Poor quality is typically related to carbonate cements in the studied sandstones from the two wells, which are developed at the depths between 2769 to 2771 m and 2775 to 2780.5 m. Moderately to strongly compacted samples taken from the depth of 2769.58 m from the first interval are mostly characterized by the high amount of ankerite and 0.2% of siderite cement. Ankerite and siderite cements fill in intergranular pores and dissolved pores and greatly destroy porosity. The lower part (2775 to 2780.5 m) is mostly characterized by the high content of calcite cement, greatly destroying porosity. This evidence exists in samples like the sample of the depth of 2779 m with its content of 30% versus the porosity of 9%. Sandstones from the sampled interval in well PY33-1-1 are characterized by low porosity and low permeability (mean value of porosity is 12% and the permeability is 33 μm^2).

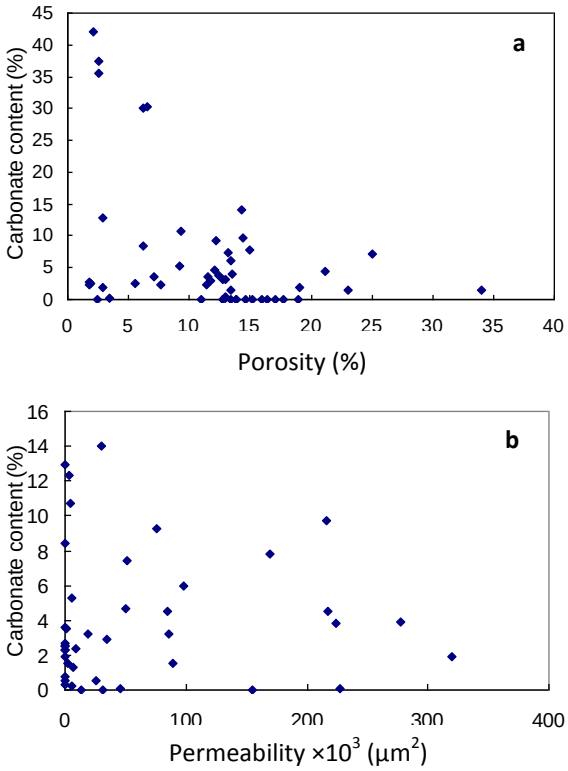

Figure 13: Reservoir quality data from the sandstones in Panyu low-uplift: (a) porosity vs. carbonate content; (b) permeability vs. carbonate content.

Sandstones from the depth of lower than 3434

m are moderately to strongly carbonate cemented (particularly calcite and ankerite cement). Ankerite cements are highly developed in the sandstones located at the depths more than 3434 m and moderately displace detrital grains. Both of them play an important role in reducing porosity in the studied intervals.

CONCLUSIONS

1- The shelf-margin deltaic sandstone reservoir of Zhuhai formation from Panyu low-uplift is fine- to medium-grained lithic sub-arkose, sub-litharenite, and sub-arkose. Major diagenesis concludes compaction, dissolution (VRF, feldspar, and carbonate cements), cementation (carbonate and quartz overgrowth), and authigenic mineral fillings (kaolinite, chlorite, illite, and smectite).

2- Compaction occurred through all the entire burial history and played a major role in porosity reduction. The effect of compaction on porosity reduction can be divided into two stages, namely eodiagenesis and meso-diagenesis. In eodiagenesis, porosity was sharply reduced because of the rearrangement of detrital grains and discharge of pore waters as compaction increased. In meso-diagenesis, porosity was stably reduced by compaction but much slower than the first stage.

3- Dissolution was the key factor that improved the reservoir quality of the shelf-margin sandstones. Dissolution began in the B stage of eodiagenesis and continued to develop in the A_2 stage of meso-diagenesis. Acidic pore fluids dissolved VRF, feldspar, and carbonate cements and generated secondary pores. Intergranular dissolution pore and intragranular dissolution pore were the main pore types in the studied area. Strong and extensively dissolution in Zhuhai formation created a secondary porosity zone in the depth interval between 2750 and 3500 m. It greatly improved reservoir quality in the studied area.

4- Carbonate cements (calcite, siderite, and ankerite) were formed early in the A stage of eodiagenesis and continued to the A_2 stage of meso-diagenesis. They played an important role in the reservoir quality evolution of shelf-margin sandstones. In eodiagenesis, carbonate cements were mainly formed which effectively prevented compacttion and the occupied pore spaces transformed into dissolution pore spaces when they were dissolved later in meso-diagenesis. Moreover, carbonate cements formed in meso-diagenesis, especially in the A_2 stage, filled in intergranular pores and dissolution pores or displaced detrital grains and greatly destroyed reservoir quality. Carbonate cements had an inverse relation-ship with reservoir quality. Generally, porosity and permeability were higher for the samples containing a smaller amount of carbonate cements.

ACKNOWLEDGMENTS

This study was jointly funded by the China National Science-Technology Project (2011 ZX05025-006) and China 973 Key Foundation Research Development Project (2009CB219400). We also express our gratitude to Shutong Li from The Key Laboratory of Petroleum Resources Research, Institute of Geology and Geophysics, and Chinese Academy of Sciences; CNOOC Research Center provided all the studied samples.

NOMENCLATURE

BS	Baiyun sag
CNOOC	China National Offshore Oil Corporation
CNPC	China National Petroleum Corporation
CUB	Central uplift belt
Ma	Million years
NUB	Northern uplift belt
PDB	Peedee Belemnite

PRMB	Pearl River Mouth Basin
QDNB	Qiongdongnan basin
SEM	Scanning electron microscope
SUB	Southern uplift belt
VRF	Volcanic rock fragments
XRD	X-ray diffraction

REFERENCES

[1] Zhang Z. T., Shi H. S., and Qing C. G. "Study on Fault Sealability of Panyu Low Massif and North Slope of Baiyun Sag," *Fault-Block Oil & Gas Field*, **2010**, *17*, 1, 24-27 (in Chinese).

[2] Zhu J. Z., Shi H. S., and Pang X., "Natural Gas Origines and Gas Source Studies of Panyu Low-uplift in Pear River Mouth Basin," *Natural Gas Geoscience*, **2005**, *16*, 4, 456-459 (in Chinese).

[3] Pittman E. D., Larese R. E., and Heald M. T., "Clay Coats: Occurrence and Relevance to Preservation of Porosity in Sandstones," *in Houseknecht D. W. and Pittman E. D., eds.*, *Origin, Diagenesis and Petrophysics of Clay Minerals in Sandstones*: *SEPM Special Publication,* **1992**, *47*, 241-264.

[4] Spötl C., Houseknecht D. W., and Longstaffe F. J., "Authigenic Chlorites in Sandstones as Indicators of High-temperature Diagenesis, Arkoma Foreland Basin, U.S.A.," *Journal of Sedimentary Research,* **1994**, *64*, 3, 553-566.

[5] Sun S. W., Shu L. S., Zeng Y. W., Cao J., et al., "Porosity-permeability and Textural Heterogeneity of Reservoir Sandstones from the Lower Cretaceous Putaohua Member of Yaojia Formation, Weixing Oilfield, Songliao Basin, Northeast China," *Marine and Petroleum Geology*, **2007,** *24*, 109-127.

[6] Zhang J. L., Jia Y., and Du G. L., "Diagenesis and its Effect on Reservoir Quality of Silurian Sandstones, Tabei Area, Tarim Basin, China," *Petroleum Science,* **2007**, *4*, 1-13 (in Chinese).

[7] Gier S., Worden R. H., Johns W. D., and Kurzweil H., "Diagenesis and Reservoir Quality of Miocene Sandstones in the Vienna Basin, Austria," *Marine and Petroleum Geology*, **2008**, *25*, 681-695.

[8] Pang X., Chen C. M., Peng D. J., Zhou D., and Chen H. H., *The Pearl River Deep-water Fan System and Petroleum in South China Sea*, Beijing: Science Press, **2007**, 6-7 (in Chinese).

[9] Ehrenberg S. N., "Preservation of Anomalously High Porosity in Deep Buried Sandstones by Grain-coating: Example from the Norwegian Continental Shelf," *AAPG Bulletin*, **1993**, *77*, 1260-1286.

[10] Mansurbega H. S., Morad A., Salem R., Marfil M. A. K., et al., "Diagenesis and Reservoir Quality Evolution of Palaeocene Deep-water, Marine Sandstones, the Shetland-faroes Basin, British Continental Shelf," *Marine and Petroleum Geology*, **2008**, *25*, 514-543.

[11] Berger A., Gier S., and Krois P., "Porosity-preserving Chlorite Cements in Shallow-marine Volcaniclastic Sandstones: Evidence from Cretaceous Sandstones of the Sawan Gas Field, Pakistan," *AAPG Bulletin*, **2009**, *93*, 5, 595-615.

[12] Zhang C. M., Li S. T., Yang J. M., Yang S. M., et al., "Petroleum Migration and Mixing in the Pearl River Mouth Basin, South China Sea," *Marine and Petroleum Geology*, **2004**, *21*, 215-224.

[13] Chen H. H., Chen C. M., Pang X., Wang J. H., et al., "Natural Gas Sources, Migration and Accumulation in the Shallow Water Area of the Panyu Lower Uplift: An Insight into the Deep Water Prospects of the Pearl River Mouth Basin, South China Sea," *Journal of Geochemical Exploration*, **2006**, *89*, 47-52.

[14] Zhou D and Yao B. C., "Tectonics and Sedimentary Basins of the South China Sea: Challenges and Progresses," *Journal of Earth Science, Printed in China*, **2009**, *20*, 1-12.

[15] Dong W., Lin C. S., and Qin C. G., "High Resolution Sequence Framework, Depositional Pattern and Litho-stratigraphic Traps of Hanjiang Formation in Panyu Uplift, Pearl River Mouth Basin,"

Geoscience, **2008**. *22*, 5, 794-801 (in Chinese).

[16] Guo X. W. and He S., "Aromatic Hydrocarbons as Indicators of Origin and Maturation for Light Oils from Panyu Lower Uplift in Pearl River Mouth Basin," *Journal of Earth Science*, **2009**, *20*, 5, 824-835 (in Chinese).

[17] Yu X. H., Jiang H and Shi H. S., "Study on Depositional Characteristic and Diagenetic Evolvement in Panyu Gas Field of Peal River Mouth Basin," *Acta Sedimentologica Sinica*, **2007**, *25*, 6, 876-884 (in Chinese).

[18] Zhu J. Z., Shi H. S and Pang X. Z., "Formation Source Rock Evaluation and Reservoired Hydrocarbon Source Analysis in the Deep-water Area of Baiyun Sag, Pearl River Mouth Basin," *China Offshore Oil and Gas*, **2008**, *20*, 223-227 (in Chinese).

[19] Wu S. G., Han Q. H., Ma Y. B., and Dong D. D., "Petroleum System in Deepwater Basins of the Northern South China Sea," *Journal of Earth Science, Printed in China*, **2009**, *20*, 124-135.

[20] Wang Q., Zhuo X. Z., Chen G. J., and Li X. Y., "Carbon and Oxygen Isotopic Composition of Carbonate Cements of Different Phases in Terrigenous Siliciclastic Reservoirs and Significance for their Origin: A Case Study from Sandstones of the Triassic Yanchang Formation, Southwestern Ordos Basin, China," *Chin. J. Geochem*, **2008**, *27*, 249-256 (in Chinese).

[21] Craig H., "The Measurement of Oxygen Isotope Paleotemperatures. In Stable Isotopes in Oceanographic Studies and Paletemperatures," *Spoleto Conference in Nuclear Geology*, *Consiglio Nazionale delle Richerche, Laboratorio di Geologia Nucleare*, Pisa, July 26-27 **1965**, 1-24.

[22] Dos Anjos S. M. C., De Ros L. F., Schiffer de Souza R., de Assis Silva C. M., et al., "Depositional and Diagenetic Controls on the Reservoir Quality of Lower Cretaceous Pendencia Sandstones, Potiguar Rift Basin, Brazil," *AAPG Bulletin*, **2008**, *84*, 1719-1742.

[23] Mackenzie F. T., "Sediments, Diagenesis, and Sedimentary Rocks," *Treatise on Geochemistry, Elsevier*, **2006**, *88*, 412-415.

[24] Xu Y. C., Liu W. H., Shen. P., and Zhang X. B., "The Evolution Characteristics and Fractionation Mechanism of Carbon Isotopes in the Process of Multi-stage Hydro-carbon Generation," *Chinese Journal of Geochemistry*, **2006**, *24*, 1-8 (in Chinese).

[25] Zhen J. J., Hu H. F., Sun G. Q., and Ji L. M., "Carbon Isotopic Characteristics of Hydrocarbon Gases from Coal-measure Source Rocks- A Thermal Simulation Experiment," **2006**, *25*, 167-172 (in Chinese).

[26] Zhang M. Q., Huang S. J., Wu Z. X., Wu S. J., et al., "Carbonate Cements and Their Formation Mechanism in Palaeogene Sandstones of Lishui Sag, East China Sea Basin," *Journal of Chengdu University of Technology (Science & Technology Edition)*, **2007**, *34*, 3, 259-266 (in Chinese).

[27] Huang S. J., Xie L. W., Zhang M., Wu W. H., et al., "Formation Mechanism of Authigenic Chlorite and Relation to Preservation of Porosity in Nonmarine Triassic Reservoir Sandstones, Ordos Basin and Sichuan Basin, China," *Journal of Chengdu University of Technology (Science &Technology Edition),* **2004**, *31*, 3, 273-281 (in Chinese).

[28] Houseknecht D. W., "Assenssing the Relative Importance of Compaction Processes and Cementation to Reduction of Porosity in Sandstones," *American Association of Petroleum Geologists Bulletin*, **1987**, *71*, 633-642.

[29] Dutton S. P., "Calcite Cement in Permian Deep-water Sandstones, Delaware Basin, West Texas: Origin, Distribution, and Effect on Reservoir Properties," *AAPG Bulletin*, **2008**, *92*, 6, 765-787.